JACS
JOURNAL OF THE AMERICAN CHEMICAL SOCIETY
Article
pubs.acs.org/JACS

Description of Aromaticity in Porphyrinoids

Judy I. Wu,*[,†] Israel Fernández,[‡] and Paul v. R. Schleyer*[,†]

[†]Department of Chemistry, Center for Computational Chemistry, University of Georgia, Athens, Georgia 30602, United States
[‡]Departamento de Química Orgánica I, Facultad de Ciencias Químicas, Universidad Complutense de Madrid, 28040, Madrid, Spain

Supporting Information

ABSTRACT: Like the larger nonplanar Möbius rings, porphyrinoid aromaticity is not due primarily to the macrocyclic π conjugation of the corresponding annulene perimeters. The block-localized wave function (BLW)-derived aromatic stabilization energies (ASE) of several porphyrinoids reveal that, on a per atom basis, the appended 6π electron heterocycles of porphyrinoids confer aromaticity much more effectively than the macrocyclic $4n+2$ π electron conjugations. There is no direct relationship between thermochemical stability of porphyrinoids and their macrocyclic $4n$ or $4n+2$ π electron counts. Porphyrinoids having an "antiaromatic" macrocyclic $4n+2$ π electron conjugation pathway (e.g., **4**) as well as those having no macrocyclic conjugation (e.g., **9**) can be stabilized by aromaticity. Computed nucleus independent chemical shifts (NICS) and the anisotropy of the induced current density (ACID) disclose the intricate local versus macrocyclic circulation interplay for several porphyrinoids.

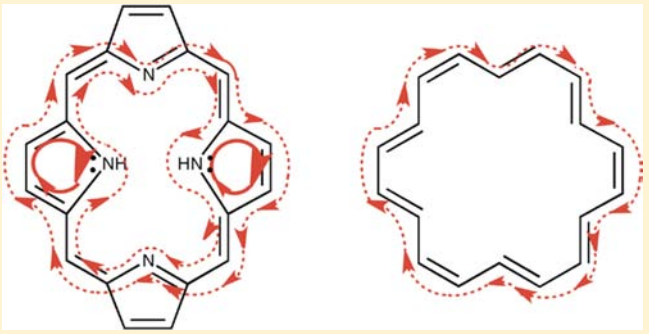

INTRODUCTION

How should aromaticity be described in porphyrins?[1] Sondheimer et al.'s synthetic [18]annulene paper[2] first noted the resemblance of the ^{1}H NMR spectra of porphyrin derivatives (δ of outer H's, +9.6 to +10.1 ppm; internal NH protons, −3.6 to −4.1 ppm)[3] to [18]annulene (δ of outer H's, +9.3 ppm; internal NH protons, −2.5 ppm).[4−6] The comment, "porphine and the derived porphyrins, as well as the phthalocyanines, are in fact the first known 18-π electron systems related to the [18]annulene,"[2] coined the popular description of porphyrins as "bridged-annulenes", and has been especially influential in the development of porphyrinoid chemistry. Vogel commented, "provided that this formal analogy exists, a symbiotic relationship between annulene and porphyrin chemistry might be established."[7]

Following Vogel's authoritative review, "The Porphyrins from the 'Annulene Chemist's' Perspective,"[8] synthetic efforts based on applying the Hückel $4n + 2$ π aromaticity rule[9] (albeit intended for monocyclic systems) to expand the porphyrin family have led to the discovery of many macrocyclic $4n + 2$ π electron conjugated porphyrins.[10] However, successful syntheses of "antiaromatic" macrocyclic [$4n$]annulenic π conjugated porphyrins, which show the opposite upfield/downfield ^{1}H NMR chemical shifts for the outer/inner protons, also are plentiful: for example, isophlorin (20 π conjugation),[11] orangarin (20 π),[12] [20]porphycene (20 π),[13] amethyrin (24 π),[12] complexed porphyrins,[14,15] thienopyrrole-containing porphyrins,[16] as well as nonplanar expanded porphyrins.[17−19] Interestingly, Kim et al. reported that the HOMO−LUMO gap for the "antiaromatic" [20]π porphycene was unexpectedly larger than its $4n + 2$ π "aromatic" congener, [18]π porphycene.[20] Along the same lines, Aihara's graph-theoretical analyses for several macrocyclic $4n$ πe conjugated porphyrins also revealed positive (aromatic) topological resonance energies.[21] Such findings contradict the Hückel $4n + 2/4n$ πe aromaticity/antiaromaticity expectation for annulenes. So are the aromaticities of porphyinoid compounds really "annulene-like"?

Unlike annulenes, the porphyrins are "decorated" with appended heterocycles and thus sustain multiple π conjugation pathways simultaneously. But how does this affect their aromaticity? Literature reports give divergent answers. Lash et al. concluded, based on comparative ^{1}H NMR and single crystal X-ray diffraction analyses of **1**−**3**, that "the aromatic characteristics of porphyrins clearly result from a number of features, but the essence of these properties appears to be encapsulated in the diaza[18]annulene substructure."[22a] On the basis of a detailed comparison of various porphyrin analogues, that is, carbaporphyrins, tropiporphyrins, azuliporphyrins, N-confused porphyrins, pyrazoloporhpyrins, and dicarbaporphyrins, Lash noted that "by taking into account hydrogen bonding, charge delocalization, steric effects, and inductive and resonance factors," the [18]annulene model "almost always predicts the correct properties for these systems."[22b] However, Sargent et al.'s ^{1}H NMR analyses of [18]porphycene and its imidazole analogues revealed that variations of the interrelationship of the induced local ("pyrrolic") versus global ("annulenic") ring currents could lead to drastically different internal NH proton

Received: September 23, 2012
Published: December 3, 2012

   dx.doi.org/10.1021/ja309434t | J. Am. Chem. Soc. 2013, 135, 315−321

shifts.[23] Isotropic nucleus independent chemical shift (NICS)[24] analyses[25,26] and computed ring currents[27] concur that both macrocyclic π conjugations and local heterocyclic π circulations contribute to the global aromaticity of porphyrinoids.[25−27] Nevertheless, how and the extent to which the imino- (NH) and ethylidene (C═C) bridges contribute to the aromaticity of porphyrins remain unclear.[1]

The C═C bonds of the dehydropyrrolic rings of **1** are usually viewed as exocyclic "ethylenic bridges" that do not participate in aromaticity.[25] Yet the influence of the pyrrolic NH's on porphyrinoid aromaticity poses interpretive challenges. On the basis of NICS analyses, Cyranski et al. concluded that "the NH groups are not inert bridging groups, as is suggested by the [18]annulene model, but instead are an integral part of the aromatic system."[25] Graph-theoretical analyses also predict the pyrrole rings to be a major source of the aromaticity of **1**.[21] Otero et al. reported that "hydrogenating a protonated pyrrole ring (of **1**)" "largely annihilates the ring current (of the corresponding dihydroporphyrin)."[27] However, Sundholm et al.'s gauge including magnetically induced current (GIMIC)[28] computations found "a larger resistance and a weaker current strength" for the pyrrolic NH units as compared to the dehydropyrrole rings of **1**.[27b]

In summarizing the disparate literature view of the origin of aromaticity in porphyrins, Bröring's seminal highlight calls for a theoretical clarification of the nature of aromatcity in porphyrins.[1] We now respond. Prior analyses based on magnetic and spectroscopic criteria have considered all possible alternatives of the origin of aromaticity in porphyrinoids, but have reached different conclusions. Our Article quantifies the energetic aspects of porphyrinoid aromaticity, based on the block-localized wave function (BLW) method,[29] for the first time. Magnetic evaluations of porphryinoid aromaticity also are discussed on the basis of their computed dissected NICS[30] and the anisotropy of the induced current density (ACID).[31]

We now seek to provide a definitive answer to how aromaticity should be described in porphyrins, and address several important questions: How and to what extent are porphyrins stabilized by aromaticity? Why are some $4n$ π electron porphyrins so viable despite their putative antiaromaticity? How do the individual local and macrocyclic π circulations (either diatropic or paratropic) of porphyrinoids influence each other and contribute to aromaticity?

RESULTS AND DISCUSSION

Large $4n + 2/4n$ π annulenes behave more like linearly conjugated olefins and are not expected to display either significant aromatic stabilization or antiaromatic destabilization per carbon.[32] Thus, the BLW-ASE's (BLW computed aromatic stabilization energies, see Computational Methods) of D_{6h} [18]annulene **7** (25.0 kcal/mol[33]) and of diaza[18]annulene **8** (26.6 kcal/mol) are only 1.4 and 1.5 kcal/mol per carbon, respectively. On the same basis, the benzene ASE (29.9 kcal/mol) is 5.0 kcal/mol per carbon.[34] Notably, the inclusion of hetero-N atoms does not perturb the aromaticity of **8**.[35] The involvement of fused azafulvene rings (denoted as "**b**" rings, see Figure 1) increases π conjugation but does not effect the aromaticity. Thus, as expected by the bridged diaza[18]-annulene nature of **3** (32.1 kcal/mol, 1.5 kcal/mol per carbon), its ASE is not much greater than **7** and **8**.[22] Clearly, the double bonds of fused dehydropyrrole rings in porphyrinoids are only inert exocyclic "bridges" and do not contribute to aromaticity.[25a]

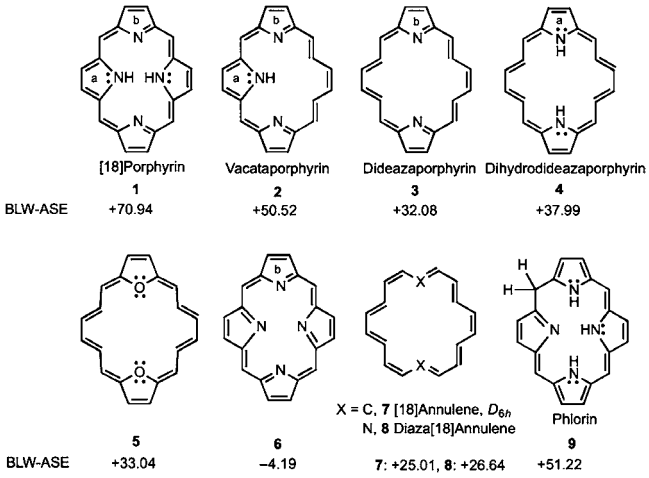

Figure 1. Block-localized wave function computed ASE's (aromatic stabilization energies, see Computational Methods) for **1**−**8** (in kcal/mol, at the B3LYP/6-31G* level). The BLW localization scheme for each structure is indicated by the resonance structure shown. The BLW-RE's for **1**−**9**, the parent pyrrole and furan rings, as well as the references used for deriving the BLW-ASE's are presented in Figures S1 and S2 in the Supporting Information (also see Computational Methods).

In sharp contrast, pyrrole-fused porphyrinoids display much greater BLW-ASE's. Thus, the ASE's of **1** (70.9 kcal/mol, 2.9 kcal/mol per carbon, two pyrrole rings) and **2** (50.5 kcal/mol, 2.4 kcal/mol per carbon, one pyrrole) are ca. 40 and 20 kcal/mol higher than **3** (32.1 kcal/mol), respectively (see Figure 1). Remarkably, the ASE's of each local 6πe pyrrole ring (ca. 20 kcal/mol each) confer almost as much aromatic stabilization as the macrocyclic 18π conjugations, for example, of **7**, **8**, and **3** (BLW-ASE's ranging from 25 to 32 kcal/mol). Based on the same BLW procedure, [18]porphycene, which also has two pyrrole rings, reveals an ASE (77.2 kcal/mol) similar to that of its structural isomer **1**.

Equations 1 and 2 evaluate the aromaticity of the fused pyrrolic rings (ca. 20 kcal/mol per ring) by comparing the energies of **1** versus **3** (eq 1, +46.5 kcal/mol) and **2** versus **3** (eq 2, +18.5 kcal/mol, one pyrrole ring in **2**) directly (B3LYP/6-31G* including ZPE). The results endorse our BLW findings quantitatively. Both eqs 1 and 2 evaluate only differences in the aromaticities of the porphryinoids on both sides of the equation. For example, in eq 2, the aromaticity of **2** (on the left) arises from both the global (18π, annulenic) and the local (6π, pyrrolic) π conjugations, but the aromaticity of **3** (on the right) comes only from the global (18π, annulenic) π conjugative circuit. The numbers and types of conjugation interactions are balanced by nonaromatic conjugated references, and the resulting energy difference (18.5 kcal/mol) estimates the pyrrolic aromatic stabilization energy of **2**.

dx.doi.org/10.1021/ja309434t | J. Am. Chem. Soc. 2013, 135, 315−321

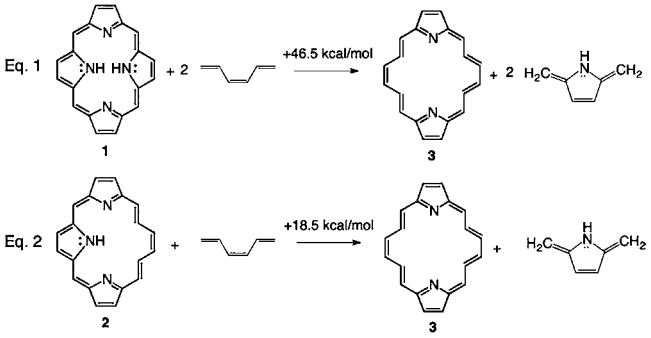

Strikingly, even $4n$ π electron porphyrinoids can be stabilized by aromaticity and have net positive ASE's when fused-pyrrole rings are involved.[21] In **4**, the ASE's of the aromatic pyrrole rings overwhelm its $4n$ π macrocyclic antiaromaticity. As a result, **4** displays a larger BLW-ASE (+38.0 kcal/mol, two pyrrole rings) than **3** (+32.1 kcal/mol), despite its magnetic "antiaromaticity" (see discussion below) and greater bond length alternation along its macrocyclic $4n$ π perimeter. Porphyrinoids with more pyrrole rings have higher ASE's and are more aromatically stabilized. This explains the peculiar viability of known Hückel antiaromatic porphyrinoids that involve either [$4n$]annulenic macrocyclic conjugations or have net $4n$ π electron counts.[11−19] Because of steric congestion between the six inner H's, the **4** minimum adopts a nonplanar geometry. This, rather than differences in aromaticity, is more likely to be responsible for the spontaneous oxidation of **4** to **3** observed experimentally.[22] Planar **5**, the minimum furan-isomer of **4**, also has a positive BLW-ASE (33.0 kcal/mol), due to the presence of two aromatic furan rings. In contrast, the $4n$ π electron **6** has four "ethylenic bridges" and reveals a small negative (destabilizing) ASE (i.e., −4.2 kcal/mol, −0.2 kcal/mol per carbon, see Figure 1), since large [$4n$]annulenic conjugations do not confer much antiaromatic destabilization.[32]

Fused sextet rings effectively increase the aromaticity of porphyrinoids, because small $4n$+2 π conjugated rings confer more aromatic stabilization than do large $4n$+2 π cycles on a per carbon basis.[9,32] But this is in addition to the overall π conjugation stabilization. ASE's measure only the extra aromatic stabilization and antiaromatic destabilization due to cyclic $4n$ + 2 π and $4n$ π conjugation. RE's measure the net stabilization due to π conjugation and thus are positive for both $4n$ and $4n$ + 2 π porphyrinoids (see Figure S1 in the Supporting Information).

Nevertheless, the spectroscopic properties (e.g., intense Soret band absorptions and characteristic ^{1}H NMR chemical shifts)[36] of porphyrins arise from their macrocyclic π conjugations. Porphyrins lacking macrocyclic π conjugations, for example, isoporphyrins, phlorin, and other calixphyrin derivatives (which have sp^3 *meso* carbon linkages), behave very differently spectroscopically.[37,38] Yet these features are not always directly linked to aromaticity.[39] Despite the absence of a macrocyclic π conjugation pathway, phlorin **9** displays a significant BLW-ASE (51.2 kcal/mol) due to its three 6 π electron aromatic pyrrole rings.

As compared to ^{1}H NMR chemical shifts, dissected NICS[30] (see Computational Methods) are superior[39] for evaluating the magnetic aromaticity of porphyrinoids. Porphyrinoids with macrocyclic $4n$+2 π (**1**, **2**, **3**) conjugations display negative total NICS(0)$_{\pi zz}$ values, while their $4n$ π congeners (**4**) show the opposite (see Figure 3). The total NICS(0)$_{\pi zz}$ is computed at the heavy atom center and includes contributions from all π and NH lone pair orbitals (see Computational Methods). However, the magnetic-based aromaticity orders of **1**−**3** and **7** do not follow their computed ASE orders (**1** > **2** > **3** > **8** ≈ **7**). The BLW-ASE of **1** is more than twice that of **3**, **7**, and **8**, but the total NICS(0)$_{\pi zz}$ values for **1** (−47.3 ppm), **2** (−42.2 ppm), **3** (−43.5 ppm), **8** (−47.2 ppm), and **7** (−47.9 ppm, computed at the D_{6h} symmetry) are all about the same. **4** is stabilized aromatically (i.e., by the two pyrrole rings) but has a positive total NICS(0)$_{\pi zz}$ value (+43.2 ppm).

Such discrepancies arise from the multifaceted nature of aromaticity, which are especially pronounced for the porphyrinoids and for other molecules with more than one fused ring. Energetic and magnetic evaluations of aromaticity are inherently different. ASE's reflect the overall energetic consequence of aromaticity (or antiaromaticity). That is, all extra cyclic stabilizing and destabilizing effects due to either the macrocyclic or the local pyrrolic conjugations are considered simultaneously. Yet magnetic assessments largely depend on the position of the "probe" used to evaluate the effect. For example, in **4** the total NICS(0)$_{\pi zz}$ is +43.2 ppm, but the local NICS(**a**)$_{\pi zz}$ is −22.8 ppm as expected by its 6 π electron pyrrolic aromaticity (see Figure 3). The local NICS(**a**)$_{\pi zz}$ is computed at the pyrrolic centers and includes only contributions from the two pyrrolic π bonds and NH lone pair (see Computational Methods).

Magnetic evaluations of porphyrinoids also are influenced by the interplay among the induced "pyrrolic" and "macrocyclic" circulations.[10g,20] As illustrated in Figure 2, the induced

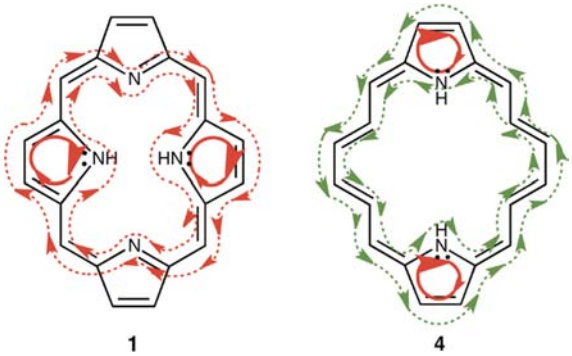

Figure 2. Schematic illustration of the local five membered ring (5MR) "pyrrolic" (solid red line) circulations and macrocyclic "annulenic" (dotted line) circulations in **1** and **4**. Diatropic/paratropic ring currents are labeled in red/green lines and are clockwise/anticlockwise (adopting the ACID convention, cf., Figure 4).

diatropic "pyrrolic" (6 π electron, solid red line) and "macrocyclic" (18 π electron, dotted red line) ring currents of **1** have opposite effects and offset each other at the pyrrolic NH lone pair regions, but accumulate at the pyrrolic double bond regions. In **4**, the macrocyclic paratropic ring current (green dotted line, see Figure 2) and the local pyrrolic diatropic ring current (solid red line, see Figure 2) vectors are opposite at the pyrrolic double bonds regions, but in the same direction at the pyrrolic NH regions.

For this reason, the pyrrolic NICS(**a**)$_{\pi zz}$ of **1** (−18.4 ppm), **2** (−21.9 ppm), and **4** (−22.8 ppm) all have reduced local NICS$_{\pi zz}$ values compared to the parent pyrrole (−33.3 ppm) (see Figure 3, **1a** and **2a**). When contributions of all of the π bonds and NH lone pairs are taken into account, the total NICS(**a**)$_{\pi zz}$ values for **1** (−33.6 ppm) and **2** (−34.6 ppm)

dx.doi.org/10.1021/ja309434t | J. Am. Chem. Soc. 2013, 135, 315−321

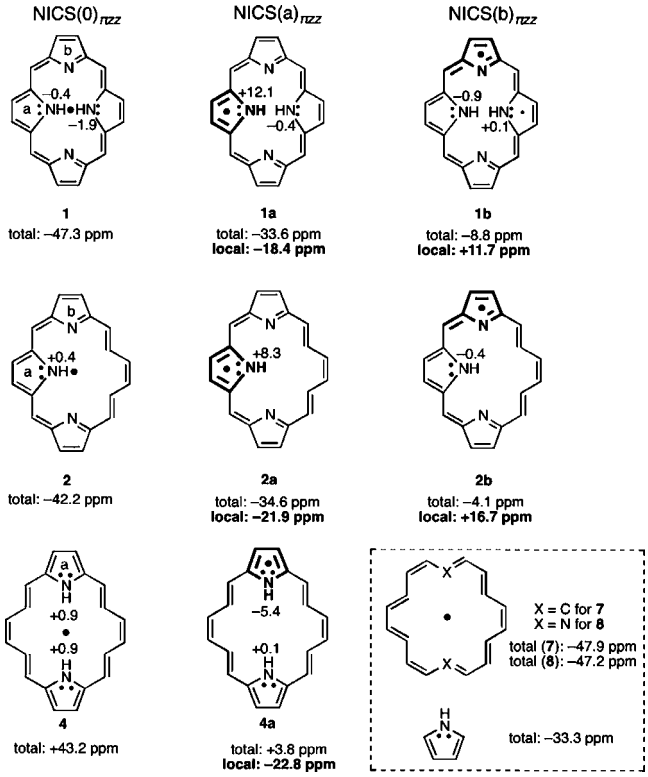

Figure 3. Dissected $NICS_{\pi zz}$ computed at the heavy atom centers "0" [$NICS(0)_{\pi zz}$], as well as at the "**a**" [$NICS(a)_{\pi zz}$] and "**b**" [$NICS(b)_{\pi zz}$] ring centers (position of NICS points indicated by the black "dots") for **1**, **2**, **4**, **7**, and **8**. The total $NICS_{\pi zz}$ include the *zz* tensor components of all π (and lone pair) MO contributions; local $NICS_{\pi zz}$ consider only contributions from the highlighted π and lone pairs MO's (in bold). Computations were performed at the PW91/IGLOIII//B3LYP/6-31G* level. (Details of the dissected NICS are presented in Figure S3 of the Supporting Information.)

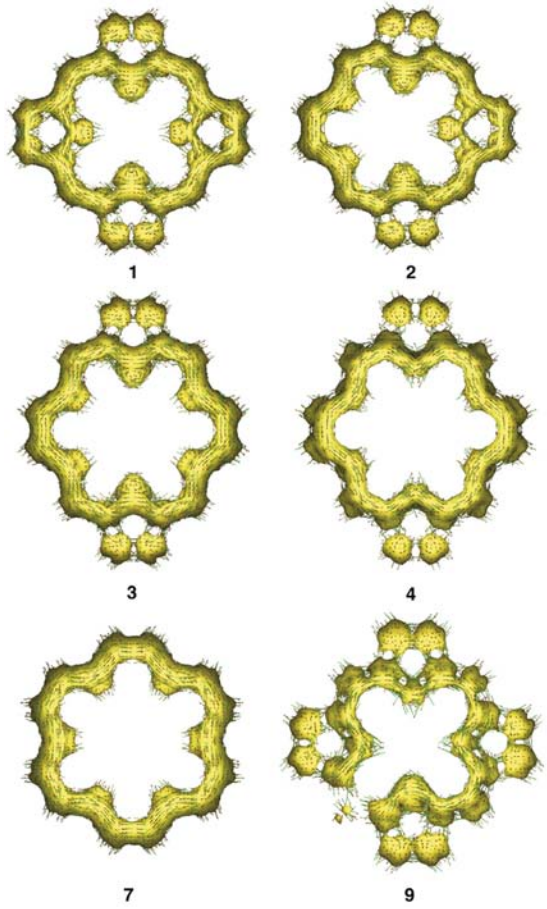

Figure 4. ACID plots at isosurface values of 0.07 for **1**−**4**, **7**, and **9**. **1**−**3** and **7** have clockwise (diatropic) macrocyclic circulations, but **4** has a counterclockwise (paratropic) macrocyclic circulation. **9** displays a "broken" counterclockwise circulation.

become more negative, as the remote double bonds of the $4n + 2$ π macrocycle contribute diatropically. In contrast, the total $NICS(\mathbf{a})_{\pi zz}$ for **4** (+3.8 ppm) becomes positive, as the remote double bonds of the $4n$ πe macrocycle contribute paratropically. The nonaromatic azafulvene "**b**" rings of **1** and **2** display moderately large positive local $NICS(\mathbf{b})_{\pi zz}$ values (**1**, +11.7 ppm; **2**, +16.7 ppm) because they reside in the deshielded region of the aromatic macrocycle (see Figure 3, **1b** and **2b**). Yet their total $NICS(\mathbf{b})_{\pi zz}$ values (−8.8 ppm for **1**, and −4.1 ppm for **2**) are small and negative due to the remote diatropic contributions from the rest of the ring. The dissected NICS of **7** and **8** do not involve such complications. In **9**, the total $NICS(\mathbf{0})_{\pi zz}$ is large and positive (+54.3 ppm), because the porphyrin center resides in the deshielded region of the three aromatic pyrrole rings (total $NICS(\mathbf{a})_{\pi zz}$= −22.7, −17.1, −17.2 ppm). Formally, **9** does not display any continuous macrocyclic π conjugation, but the *meso* CH_2 group can involve hyperconjugatively[40] with the π conjugation in the system resulting in pseudo 20 π electron antiaromaticity. The nonaromatic "**b**" ring displays a small negative total $NICS(\mathbf{b})_{\pi zz}$ value (−3.6 ppm).

Details of the ACID[31] plots support our NICS findings (see Figure 4). In **1** and **2**, the induced current density vectors are clockwise (diatropic) at the pyrrolic double bond regions, but the vector directions at the NH lone pair regions are counterclockwise (paratropic) with respect to the pyrrole ring. The exocyclic "ethylenic bridges" of the azafulvene rings in **1**, **2**, and **3** reveal only local circulations. This is in sharp contrast with the continuous diatropic ACID surfaces of **7** (see Figure 4). The ACID plot of **4** displays a dominating counterclockwise circulation due to its macrocyclic 20 π electron conjugation. Compound **9** behaves similar to **4** but has a "broken" counterclockwise circulation due to its saturated *meso* CH_2 group. The contrasting macrocyclic (paratropic) and local (diatropic) π circulations in both **4** and **9** offset each other at the pyrrolic double bond regions, but circulate in the same direction at the NH lone pair regions.

■ CONCLUSIONS

Although energetic and magnetic aromaticity measures agree generally for monocyclic compounds,[41] the aromaticities of porphyrins and other polycyclic conjugated systems are particularly "multifaceted". For the porphyrins, the ASE's arising from macrocyclic and local π circulations contribute collectively to the total aromatic stabilization energy ($4n$ π electron conjugations contribute negative ASE's and are destabilizing). Yet magnetic-based evaluations of aromaticity largely depend on the position of the "probe" used to evaluate the effect and are strongly influenced by the (constructive or destructive) interference between multiple $4n$+2 πe and $4n$ πe conjugation circuits at various regions of the molecule.

The "bridged annulene" view of porphyrins does not describe their aromaticity sufficiently. Instead, the appended 6π aromatic

sextets confer aromaticity much more effectively than macrocyclic $4n + 2$ π electron conjugations. This explains the unexpected viability of many porphyrinoids with "antiaromatic" macrocyclic $4n$ π electron conjugation pathways and provides and effective strategy for stabilizing larger porphyrinoids. But the porphyrinoids are not unique in this sense. The aromaticity of many fused ring systems also appears to arise mainly from their small fused aromatic rings rather than the macrocyclic conjugations, for example, in the large nonplanar Möbius cycles.[42] In essence, this agrees with the Hückel expectation, that small $4n + 2$ πe conjugated rings confer more aromatic stabilization (per carbon) than do large $4n + 2$ πe cycles.[9,32]

COMPUTATIONAL METHODS

All geometries were optimized at the B3LYP/6-31G* level as implemented in Gaussian 03.[43] Vibrational frequency computations verified the nature of the stationary points. **1**, **2**, **3**, **5**, **6**, **7** (D_{6h}[44]), and **8** have planar minimum geometries. Because of significant steric repulsion between the inner H's, both **4** and **9** have nonplanar minima that are 1.62 and 7.69 kcal/mol lower in energy than their planar forms (NIm = 4 for **4**, and NIm = 3 for **9**). The planar forms of all compounds were adopted for the BLW, NICS, and ACID computations.

Nucleus independent chemical shifts (NICS) computations,[30] based on the individual gauge for localized orbitals (IGLO) method[44] (implemented in the deMon NMR program),[45] were performed at the PW91/IGLOIII level employing the Pipek−Mezey localization algorithm.[46] We employ the most sophisticated $NICS_{\pi zz}$ index, which extracts the out-of-plane (zz) tensor component of the isotropic NICS and includes only selected π MO contributions. The total $NICS_{\pi zz}$ include contributions from all π and NH lone pair orbitals. Local $NICS_{\pi zz}$ include contributions from only the π (including NH lone pair, if any) orbitals directly associated with a particular ring moiety (bold in Figure 3). Dissected $NICS_{\pi zz}$ for **1**, **2**, **4**, **7**, **8**, and **9** were computed at: (1) the heavy atom centers, NICS(0), (2) the pyrrolic ring centers, NICS(**a**), and (3) the azafulvene ring centers, NICS(**b**). Negative/positive $NICS(0)_{\pi zz}$ computed at ring centers denote aromaticity/antiaromaticity. However, NICS analyses of the porphyrins are complicated by the involvement of multiple cyclic circulations (either paratropic, diatropic, or both) and require more careful interpretation. The anisotropy of the induced current density (ACID) method[31] was employed complimentarily to visualize the induced delocalization of π electrons.

The block localized wave function (BLW) method[29] was employed to evaluate the RE's and the ASE's of **1**−**9** at the B3LYP/6-31G* level (as implemented in GAMESS R5 version).[47] The molecular orbital MO-based computational procedure of the BLW method preserves the concepts of ab initio valence bond (VB) theory, but is practicable for studying large molecular systems.[33,48] Following the Pauling−Wheland RE definition,[49] BLW-RE's are based on the difference between the energy of the completely optimized fully delocalized structure Ψ^{deloc} of the target molecule and that of its most stable hypothetical resonance structure Ψ^{loc} (optimized under the BLW constraint). The latter is constructed by partitioning all of the electrons and basis functions into several subspaces to form sets of localized MO's, in which orbitals of the same subspaces are mutually orthogonal but orbitals of different subspaces overlap freely. This procedure "disables" the intramolecular interactions among the selected subgroups. Note that **2** and **4** have two difference resonance contributors (corresponding to two different localization schemes). For such cases, the average BLW-RE of both localization schemes was applied.

The BLW-ASE's are based on the BLW-RE differences between the target aromatic/antiaromatic molecule and acyclic conjugated reference species with the same number and types of conjugations (see below).[50] Note that RE's measure the overall π conjugation stabilization, but ASE's evaluate the extra stabilization (or destabilization) associated with aromaticity (or antiaromaticity), and thus differ conceptually. By definition, the RE's are always positive, but the ASE's can be either positive (indicating aromaticity) or negative (indicating antiaromaticity). For example, the BLW-ASE of **7** (+25.0 kcal/mol) is evaluated by its BLW-RE (129.7 kcal/mol) as compared to that of six *anti*-butadienes (BLW-RE = 12.2 kcal/mol each) and three *syn*-butadienes (BLW-RE = 10.5 kcal/mol each). The BLW-RE's for all reference compounds are listed in Figure S2 in the Supporting Information.

DFT methods, in particular the popular B3LYP functional, are known to be problematic for evaluating the relative energies of annulene isomers[51,52] by overestimating the effects of electron delocalization. However, errors due to such methodological imperfections are minimized for the BLW-ASE comparisons, which are based on relative (BLW-RE) energy differences between data computed at the same theoretical level. Although concerns regarding the nonorthogonal partitioning of basis functions of the BLW method have been raised,[53] such misgivings do not compromise the validity of judiciously obtained BLW results (for a more technical discussion, see ref 54, Methods section, and ref 55). Computed BLW delocalization energies fluctuate only slightly among different midsize basis sets,[55] and more importantly agree well with viable experimental estimates. For example, the computed BLW-RE (61.4 kcal/mol)[50] and BLW-ASE (29.9 kcal/mol)[50] of benzene at the B3LYP/6-31G* level, evaluated by the same procedure employed here, is in excellent agreement with the best RE (65.1 kcal/mol)[56] and ASE (28.8 kcal/mol)[56] values derived from experimental data.[33]

ASSOCIATED CONTENT

Supporting Information

Computed BLW-RE's for **1**−**8** and reference compounds for deriving BLW-ASE's, dissected NICS data for **1**, **2**, **4**, **7**, **8**, and **9**, and B3LYP/6-31G* optimized coordinates for **1**−**9**. This material is available free of charge via the Internet at http://pubs.acs.org.

AUTHOR INFORMATION

Corresponding Author

judywu@uga.edu; schleyer@chem.uga.edu

Notes

The authors declare no competing financial interest.

ACKNOWLEDGMENTS

This work was supported by the USA NSF grant CHE-105-7466. I.F. thanks the Spanish MICINN and CAM (Grant no. CTQ2010-20714-C02-01, Consolider-Ingenio CSD2007-00006, S2009/PPQ-1634, and a Ramón y Cajal contract) for financial support. We thank Clémence Corminboeuf for helpful discussions and the referees for constructive comments.

REFERENCES

(1) Bröring, M. *Angew. Chem., Int. Ed.* **2011**, *50*, 2436−2438.
(2) Sondheimer, F.; Wolovsky, R.; Amiel, Y. *J. Am. Chem. Soc.* **1962**, *84*, 274−284.
(3) (a) Becker, E. D.; Bradley, R. B. *J. Chem. Phys.* **1959**, *31*, 1413. (b) Ellis, J.; Jackson, A. H.; Kenner, G. W.; Lee, J. *Tetrahedron Lett.* **1960**, *2*, 23.
(4) Stökel, K.; Sondheimer, F. *Org. Synth. Coll.* **1988**, *6*, 68.
(5) Oth, J. F. M. *Pure Appl. Chem.* **1971**, *25*, 573−622.
(6) Stevenson, C. D.; Kurth, T. L. *J. Am. Chem. Soc.* **2000**, *122*, 722−723.
(7) Vogel, E. *Angew. Chem., Int. Ed.* **2011**, *50*, 4278−4287.
(8) Vogel, E. *Pure Appl. Chem.* **1993**, *65*, 143−152.
(9) Hückel, E. *Z. Phys.* **1931**, *70*, 204−286.
(10) (a) Sessler, J. L.; Gebauer, A.; Vogel, E. *The Porphyrin Handbook*; Academic Press: New York, 2000; Vol. 2, p 1. (b) Vogel, E. *Pure Appl. Chem.* **1996**, *68*, 1355−1360. (c) Fleischer, E. B. *Acc. Chem. Res.* **1970**, *3*, 105−112. (d) Vogel, E. *J. Heterocycl. Chem.* **1996**, *33*,

1461−1487. (e) Pacholska, E.; Latos-Grazynski, L.; Ciunik, Z. *Chem.-Eur. J.* **2002**, *8*, 5403−5405. (f) Vaid, T. P. *J. Am. Chem. Soc.* **2011**, *133*, 15838−15841. (g) Okujima, T.; Kikkawa, T.; Nakano, H.; Kubota, H.; Fukugami, N.; Ono, N.; Yamada, H.; Uno, H. *Chem.-Eur. J.* **2012**, *18*, 12854−12863.
(11) Liu, C.; Shen, D. M.; Chen, Q. Y. *J. Am. Chem. Soc.* **2007**, *129*, 5814−5815.
(12) Sessler, J. L.; Weghorn, S. J.; Hiseada, Y.; Lynch, V. *Chem.-Eur. J.* **1995**, *1*, 56−67.
(13) Hayashi, T.; Nakashima, Y.; Ito, K.; Ikegami, T.; Aritome, I.; Suzuki, A.; Hisaeda, Y. *Org. Lett.* **2003**, *5*, 2845−2848.
(14) Kakui, T.; Sugawara, S.; Hirata, Y.; Kojima, S.; Yamamoto, Y. *Chem.-Eur. J.* **2011**, *17*, 7768−7771.
(15) (a) Cissel, J. A.; Vaid, T. P.; Yaps, G. P. A. *Org. Lett.* **2006**, *8*, 2401−2404. (b) Cissel, J. A.; Vaid, T. P.; Rheingold, A. L. *J. Am. Chem. Soc.* **2005**, *127*, 12212−12213.
(16) Chang, Y.; Chen, H.; Zhou, Z.; Zhang, Y.; Schütt C.; Herges, R.; Shen, Z. *Angew. Chem., Int. Ed.* **2012**, *51*, DOI: 10.1002/anie.201204954.
(17) (a) Saito, S.; Osuka, A. *Angew. Chem., Int. Ed.* **2011**, *50*, 4242−4253. (b) Mori, H.; Sung, Y. M.; Lee, B. S.; Kim, D.; Osuka, A., *Angew. Chem., Int. Ed.* **2012**, *51*, DOI: 10.1002/anie.201207212.
(18) (a) Stepien, M.; Latos-Grazynski, L.; Sprutta, N. *Angew. Chem., Int. Ed.* **2011**, *50*, 4288−4340. (b) Stepien, M.; Latos-Grazynski, L.; Sprutta, N.; Chwalisz, P.; Szterenberg, L. *Angew. Chem., Int. Ed.* **2007**, *46*, 7869−7873.
(19) Sessler, J. L.; Seidel, D. *Angew. Chem., Int. Ed.* **2003**, *42*, 5134−5175.
(20) Kim, K. S.; Sung, Y. M.; Matsuo, T.; Hayashi, T.; Kim, D. *Chem.-Eur. J.* **2011**, *17*, 7882−7889.
(21) (a) Aihara, J.-i.; Kimura, E.; Krygowski, T. M. *Bull. Chem. Soc. Jpn.* **2008**, *81*, 826−835. (b) Aihara, J.-i. *J. Phys. Chem. A* **2008**, *112*, 5305−5311. (c) Aihara, J.-i.; Makino, M. *Bull. Chem. Soc. Jpn.* **2009**, *82*, 675−682. (d) Aihara, J.-i.; Makino, M. *Org. Biomol. Chem.* **2010**, *8*, 261−266. (e) Aihara, J.-i.; Nakagami, Y.; Makino, M. *J. Phys. Chem. A* **2012**, DOI: 10.1021/jp310480d.
(22) (a) Lash, T. D.; Jones, S. A.; Ferrence, G. M. *J. Am. Chem. Soc.* **2010**, *132*, 12786−12787. (b) Lash, T. D. *J. Porphyrins Phthalocyanines* **2011**, *15*, 1093−1115. (c) Lash, T. D.; Hayes, M. J. *Angew. Chem., Int. Ed. Engl.* **1997**, *36*, 840−842. (d) Lash, T. D.; Romanic, J. L.; Hayes, M. J. *Chem. Commun.* **1999**, 819−820.
(23) Sargent, A. L.; Hawkins, I. C.; Allen, W. E.; Liu, H.; Sessler, J. L.; Fowler, C. J. *Chem.-Eur. J.* **2003**, *9*, 3065−3072.
(24) (a) Schleyer, P. v. R.; Maerker, C.; Dransfeld, A.; Jiao, H. J.; Hommes, N. J. r. V. E. *J. Am. Chem. Soc.* **1996**, *118*, 6317−6318. (b) Schleyer, P. v. R.; Jiao, H. J.; Hommes, N. J. r. V. E.; Malkin, V. G.; Malkina, O. L. *J. Am. Chem. Soc.* **1997**, *119*, 12669−12670.
(25) (a) Cyranski, M. K.; Krygowski, T. M.; Wisiorowski, M.; Hommes, N. J. R. v. E.; Schleyer, P. v. R. *Angew. Chem., Int. Ed.* **1998**, *37*, 177−180. (b) Krygowski, T. M.; Cyranski, M. K. *Chem. Rev.* **2001**, *101*, 1385−1419.
(26) (a) Jusélius, J.; Sundholm, D. *J. Org. Chem.* **2000**, *65*, 5233−5237. (b) Jusélius, J.; Sundholm, D. *Phys. Chem. Chem. Phys.* **2000**, *2*, 2145−2151.
(27) (a) Otero, N.; Fias, S.; Radenković, S.; Bultinck, P.; Graña, A. M.; Mandado, M. *Chem.-Eur. J.* **2011**, *17*, 3274−3286. (b) Fliegl, H.; Sundholm, D. *J. Org. Chem.* **2012**, *77*, 3408−3414. (c) Steiner, E.; Fowler, P. W. *Org. Biomol. Chem.* **2006**, *4*, 2473−2476. (d) Steiner, E.; Soncini, A.; Fowler, P. W. *Org. Biomol. Chem.* **2005**, *3*, 4053−4059. (e) Steiner, E.; Fowler, P. W. *Org. Biomol. Chem.* **2003**, *1*, 1785−1789. (f) Steiner, E.; Fowler, P. W. *ChemPhysChem* **2002**, *3*, 114−116.
(28) Fliegl, H.; Taubert, S.; Lehtonen, O.; Sundholm, D. *Phys. Chem. Chem. Phys.* **2011**, *13*, 20500−20518.
(29) (a) Mo, Y.; Peyerimhoff, S. D. *J. Chem. Phys.* **1998**, *109*, 1687−1697. (b) Mo, Y.; Song, L.; Lin, Y. *J. Phys. Chem. A* **2007**, *111*, 8291−8301.
(30) (a) Corminboeuf, C.; Heine, T.; Seifert, G.; Schleyer, P. v. R. *Phys. Chem. Chem. Phys.* **2004**, *6*, 273−276. (b) Fallah-Bagher-Shaidaei, H.; Wannere, C. S.; Corminboeuf, C.; Puchta, R.; Schleyer, P. v. R. *Org. Lett.* **2006**, *8*, 863−866. (c) Chen, Z.; Wannere, C. S.; Corminboeuf, C.; Puchta, R.; Schleyer, P. v. R. *Chem. Rev.* **2005**, *105*, 3842−3888.
(31) (a) Herges, R.; Geuenich, D. *J. Phys. Chem. A* **2001**, *105*, 3214−3220. (b) Geuenich, D.; Hess, K.; Köhler, F.; Herges, R. *Chem. Rev.* **2005**, *105*, 3758−3772. ACID calculations have been used in the analysis of various planar and nonplanar porphyrinoids because they reveal the induced ring current density expected when an external magnetic field is applied; see refs 16 and 31b
(32) (a) Longuet-Higgins, H. C.; Salem, L. *Proc. R. Soc.* **1959**, *251*, 172−185. (c) Coulson, C. A.; Dixon, W. T. *Tetrahedron* **1962**, *17*, 215−228. (b) Wannere, C. S.; Schleyer, P. v. R. *Org. Lett.* **2003**, *5*, 865−868.
(33) The BLW-ASE (25.0 kcal/mol) and computed isomerization stabilization energy (27.4 kcal/mol, see ref 32b) of D_{6h} **7** are in reasonable agreement; this supports our use of the BLW procedure.
(34) Wu, J. I.; Wannere, C. S.; Mo, Y.; Schleyer, P. v. R.; Bunz, U. H. F. *J. Org. Chem.* **2009**, *74*, 4343−4349.
(35) Wang, Y.; Wu, J. I.; Li, Q. S.; Schleyer, P. v. R. *Org. Lett.* **2010**, *12*, 4824−4827.
(36) Gellini, C.; Salvi, P. R. *Symmetry* **2010**, *2*, 1846−1924 and references therein.
(37) (a) Kadish, K. M.; Smith, K. M.; Guilard, R. *The Porphyrin Handbook: NMR and EPR*; Academic Press: New York, 1999; Vol. *5*, p 23. (b) Dolphin, D.; Felton, R. H.; Borg, D. C.; Fajer, J. *J. Am. Chem. Soc.* **1970**, *92*, 743−745. The ^{1}H NMR shifts for the outer pyrrole protons of **1** (ranging from +9.9 to +11.2 ppm) and those of the isoporphyrin derivatives (ranging from +6.2 to +6.5 ppm) differ drastically. Isoporphyrins also do not exhibit the characteristic Soret and Q bands of "annulene-like" porphyrins, but absorb at longer wavelengths (ca. 800 nm).
(38) (a) Abraham, R. J.; Smith, K. M.; Goff, D. A.; Lai, J.-J. *J. Am. Chem. Soc.* **1982**, *104*, 4432−4437. (b) Katz, J. J. In *Porphyrins and Metallaporphyrins*; Smith, K. M., Ed.; Elsevier: Amsterdam, 1975; p 442.
(39) Wannere, C. S.; Corminboeuf, C.; Allen, W. D.; Schaefer, H. F., III; Schleyer, P. v. R. *Org. Lett.* **2005**, *7*, 1457−1460. The downfield ^{1}H NMR chemical shifts of polycyclic unsaturated non-aromatic hydrocarbons are the result of their extensive π conjugation rather than aromaticity.
(40) (a) Nyulaszi, L.; Schleyer, P. v. R. *J. Am. Chem. Soc.* **1999**, *121*, 6872−6875 and references cited. (b) Herrero-García, N.; Fernández, I.; Osío-Barcina, J. *Chem.-Eur. J.* **2011**, *17*, 7327−7335 and references therein.
(41) (a) Wang, Y.; Fernández, I.; Duvall, M.; Wu, J. I.; Li, Q.; Frenking, G.; Schleyer, P. v. R. *J. Org. Chem.* **2010**, *75*, 8252−8257. (b) Fernández, I.; Duvall, M.; Wu, J. I.; Schleyer, P. v. R.; Frenking, G. *Chem.-Eur. J.* **2011**, *17*, 2215−2224.
(42) Castro, C.; Chen, Z. F.; Wannere, C. S.; Jiao, H.; Karney, W. L.; Mauksch, M.; Puchta, R.; Hommes, N. J. R. v. E.; Schleyer, P. v. R. *J. Am. Chem. Soc.* **2005**, *127*, 2425−2432.
(43) Frisch, M. J.; et al. *Gaussian 03*, revision C.02; Gaussian, Inc.: Wallingford, CT, 2004. See complete reference in the Supporting Information.
(44) Fleischer, U.; Kutzelnigg, W.; Lazzeretti, P.; Mühlenkamp, V. *J. Am. Chem. Soc.* **1994**, *116*, 5298−5306 and references cited therein.
(45) Malkin, V. G.; Malkina, O. L.; Casida, M. E.; Salahub, D. R. *J. Am. Chem. Soc.* **1994**, *116*, 5898−5908.
(46) Pipek, J.; Mezey, P. J. *J. Chem. Phys.* **1989**, *90*, 4916−4927.
(47) Gamess (Version R5): Schmidt, M. W.; Baldridge, K. K.; Boatz, J. A.; Elbert, S. T.; Gordon, M. S.; Jensen, J. H.; Koseki, S.; Matsunaga, N.; Nguyen, K. A.; Su, S. J.; Windus, T. L.; Dupuis, M.; Montgomery, J. A. *J. Comput. Chem.* **1993**, *14*, 1347−1363.
(48) Wu, J. I.; Dobrowolski, M. A.; Cyranski, M. K.; Merner, B. L.; Bodwell, G. J.; Mo, Y.; Schleyer, P. v. R. *Mol. Phys.* **2009**, *107*, 1177−1186.
(49) (a) Pauling, L. C.; Wheland, G. W. *J. Chem. Phys.* **1933**, *1*, 362−374. (b) Pauling, L. C. *The Nature of the Chemical Bond*, 3rd ed.; Cornell University Press: Ithaca, NY, 1960. (c) Wheland, G. W. *J. Am.*

Chem. Soc. **1941**, *85*, 431−434. (d) Wheland, G. W. *The Theory of Resonance*; Wiley: New York, 1944. (e) Wheland, G. W. *Resonance in Organic Chemistry*; Wiley: New York, 1955.
(50) Mo, Y.; Schleyer, P. v. R. *Chem.-Eur. J.* **2006**, *12*, 2009−2020.
(51) Both BHLYP and KMLYP methods predict D_{6h} **7** to be a transition structure (NIm = 1), 3.2 and 2.6 kcal/mol higher in energy than the C_2 minimum. The computed NMR properties of C_2 **7** also agree better with experiment. See also: Wannere, C. S.; Sattelmeyer, K. W.; Schaefer, H. F., III; Schleyer, P. v. R. *Angew. Chem., Int. Ed.* **2004**, *43*, 4200−4206.
(52) King, R. A.; Crawford, T. D.; Stanton, J. F.; Schaefer, H. F., III. *J. Am. Chem. Soc.* **1999**, *121*, 10788−10793.
(53) Zielinski, M.; Havenith, R. W. A.; Jenneskens, L. W.; Lenthe, J. H. v. *Theor. Chem. Acc.* **2010**, *127*, 19−25.
(54) Wu, J. I.; Fernández, I.; Mo, Y.; Schleyer, P. v. R. *J. Chem. Theory Comput.* **2012**, *8*, 1280−1287.
(55) Mo, Y.; Hiberty, P. C.; Schleyer, P. v. R. *Theor. Chem. Acc.* **2010**, *127*, 27−38.
(56) Cyranski, M. K. *Chem. Rev.* **2005**, *105*, 3773−3811.